

## ii. Insertions

The insertions serve two functions: they transport the beams from arc to arc, and they control the lattice parameters at the crossing points. For injection, we require a  $\beta^*$  at the crossing point where all the  $\beta$ 's throughout the insertion are small,  $\beta^* = 10$  m was found to be a good choice. During experiments, the smallest practical  $\beta^*$  would lead to the largest luminosities. This leads to the  $\beta$  function range at the crossing point of  $\beta^* = \beta_H^* = \beta_V^* \approx 1-10$  m. Furthermore, the crossing angle is adjustable from  $\alpha \approx 0-7.7$  mrad. Note, the actual range is limited by the aperture of the DX dipole.

As the insertion is tuned, the phase advance across the insertion changes as well. This can create a mismatch when each insertion is tuned to a different  $\beta^*$ . The worst case situation is when one insertion is at  $\beta^* = 1$  m and 5 insertions are at  $\beta^* = 10$  m, then  $\Delta\beta/\beta, \Delta X_p/X_p < 5\%$ . Since  $a_1$  and  $b_1$  errors could cause a larger ripple, this may be of little consequence. However, the ripple can be reduced by tuning the lattice differently, such as imposing fixed phase advance across the insertion, etc.

Figure 11-4 shows the half-insertion at 6 o'clock and Fig. 11-5 an expanded layout of an insertion on one side of the interaction point. Each half-insertion is composed of (1) a dispersion matching section (D9, Q9, D8, Q8, Q7, D6, Q6 and D5); (2) a straight betatron function matching section ("telescope") with the quadrupole doublet Q5, Q4 and the triplet Q3, Q2 and Q1; and (3) the beam crossing dipoles D0 and DX. D5 of the inner and outer half-insertions serve also to bring the beam-beam separation from 90 cm to 41.5 cm at the edge of D0. The magnets D6 and D9 are identical with a magnet length of 2.95 m. The insertion dipoles D8 are identical to the arc dipoles, and D0 has a magnetic length of 3.6 m. The magnets Q3, Q2, Q1, and D0 of inner and outer insertions sit in common vacuum vessels. The large aperture dipole DX is common to both rings, but electrically and cryo connected to the blue ring. The dipole DX, as well as D0 in the insertions, are separately adjustable to allow for unequal species or finite crossing angle operation.

The dipoles D0, D6 and D9 are assumed to be curved. However, if any of these dipoles are manufactured as straight, additional correction is required. An adequate correction scheme was found by adding shunt correction supplies to Q1, Q7 and on the trims of Q5 and Q6 where  $\Delta G/G \sim 0.1\%$ .

Note, Q9I is identical to Q8O and they are sometimes denoted as QFA in lattice calculations. Similarly, Q8I and Q9O are also referred to as QDA.

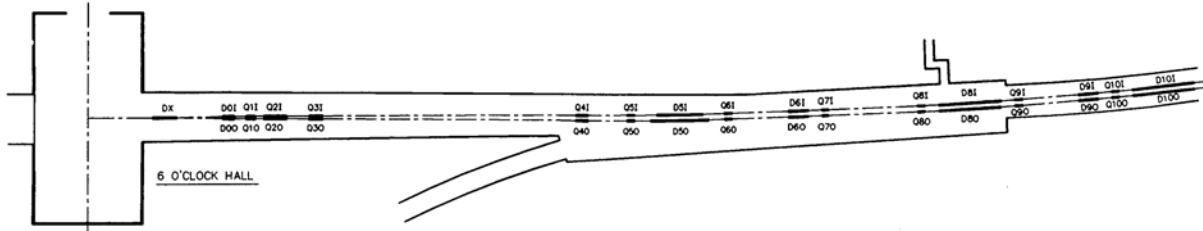


Fig. 11-4. RHIC half-insertion at 6 o'clock.

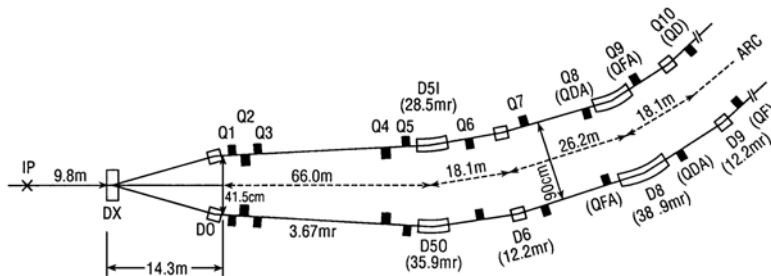


Fig. 11-5. Expanded layout of half-insertion.



insertion are given in Table 11-2, and the behaviors of the betatron and dispersion functions are shown in Fig. 11-6.

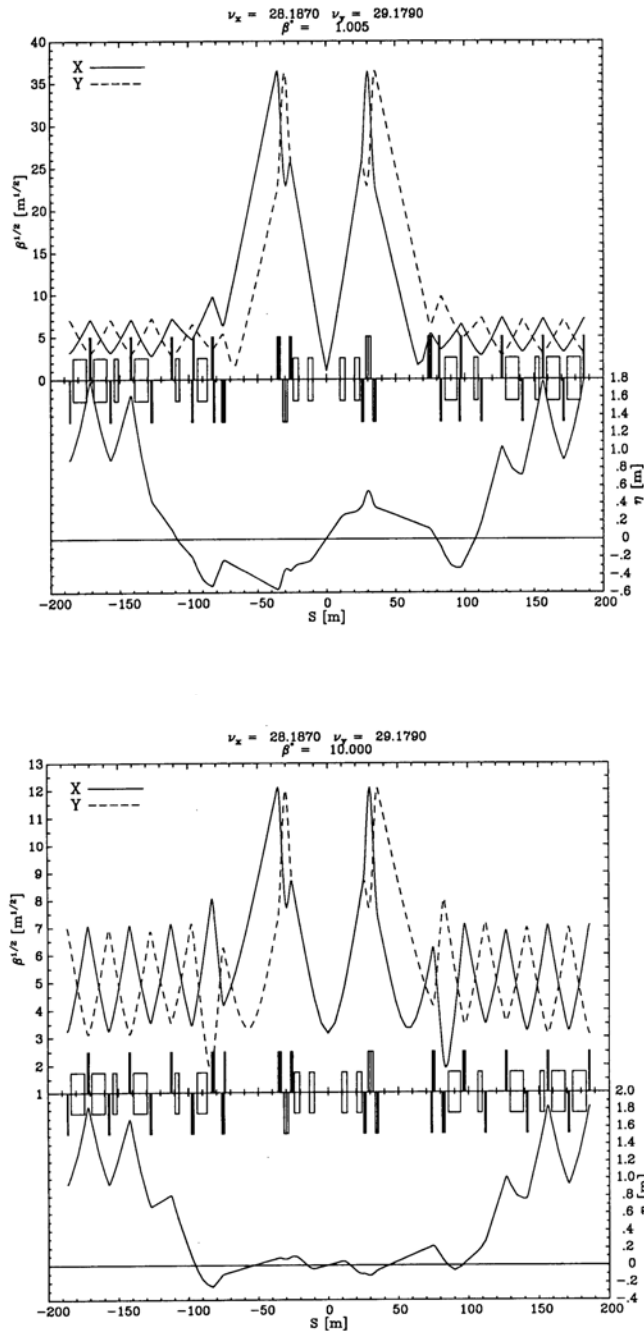
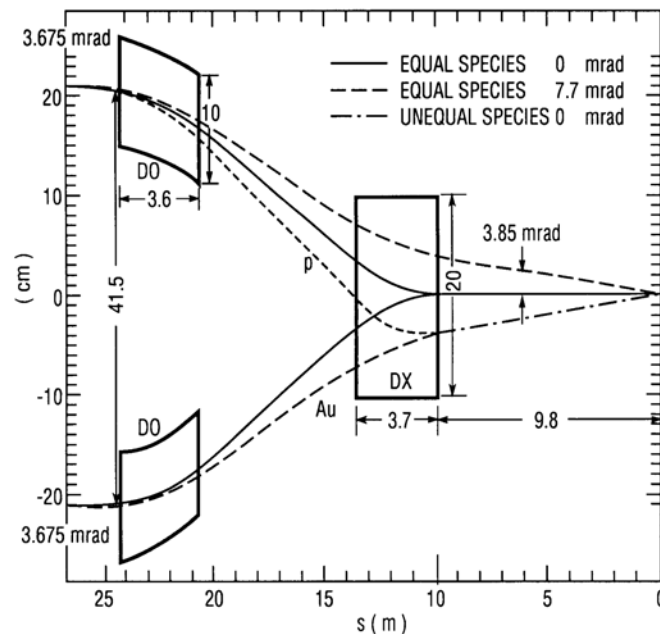


Fig. 11-6. Betatron and dispersion functions in the insertion region.

The beam crossing geometry is shown in Fig. 11-7. DX is common to both beams, D0 of inner and outer insertions are separately excited to accommodate variations in beam crossing angles as well as collisions between unequal species. For unequal species, such as p on Au, the line of head-on collision is rotated by about 3.85 mrad with respect to the longitudinal center axis. For nonzero-angle collisions the insertion quadrupoles have to be readjusted in strength by less than 1% in order to preserve the dispersion characteristics.

The dynamic aperture in the low  $\beta^*$  configuration is dominated by the coil radius of the high-beta quadrupoles Q1, Q2, Q3 and D0 dipole. Since the large-aperture quadrupoles are frozen at 13 cm coil i.d. by available tooling, the "matched" aperture of D0 would be  $(\beta @ D0/\beta @ Q3)^{1/2} \times 13 \text{ cm} \approx 8.7 \text{ cm}$ . Tracking studies suggest that the dynamic aperture can be increased with a D0 aperture of 10 cm. In order to accommodate yoke dimensions, D0 cannot be placed any closer than the 7 m to DX as shown in Fig. 11-7. A summary of major lattice dipole and quadrupole parameters is given in Table 11-3.



**Fig. 11-7.** Beam crossing geometry (magnetic lengths are shown).

**Table 11-3.** Summary of Dipole and Quadrupole Parameters

	Coil i.d. (mm)	Eff. Length (m)	Field @ 100 GeV/u <sup>†</sup> (T;T/m)		Location Number	
DIPOLES	80	9.45**	3.45		ARC, D8	288
	80	2.95	3.45		D6, D9	48
	80	8.71	3.45		D5O	12
	80	6.92	3.45		D5I	12
	Subtotal, 80 mm					360
	100	3.60	3.52		D0	24
	200	3.70	4.27		DX	12
QUADRUPOLES			$\beta^*=10$ m	$\beta^*=1$ m		
	80	1.11	68.2	69.5	QF	138
	80	1.11	70.5	71.8	QD	138
	80	1.11	65.4	73.5	QFA (Q9I, Q8O)	24
	80	1.11	66.4	74.6	QDA (Q9O, Q8I)	24
	80	1.11	75.5	75.5	Q5, Q6 <sup>¶</sup>	48
	80	0.93	76.3	72.0	Q7	24
	80	1.81	75.5	75.5	Q4 <sup>¶</sup>	24
	Subtotal, 80 mm					420
	130	1.44	46.7	48.5	Q1	24
	130	3.40	46.3	47.1	Q2	24
	130	2.10	46.0	47.3	Q3	24
Subtotal, 130 mm						<u>72</u>
TOTAL, dipole and quadrupole magnets						888

\*\*physical length 9.728 m (383.0 in.)

<sup>†</sup> Quench field in

80 mm Dipole 4.6 T

100 mm Dipole 4.42 T

200 mm Dipole 5.14 T

80 mm Quad 107 T/m

130 mm Quad 75.3 T/m

<sup>¶</sup> Trim quadrupoles at Q4, Q5, Q6 provide gradient changes from  $\beta^* = 10$  to 1 m.

Injection into the collider, acceleration and low-energy operation will be done with the  $\beta^* = 10$  m configuration. The low-beta configuration with  $\beta^* = 1$  m can be obtained at high energies, nominally above 30 GeV/u, by changing the insertion quadrupole excitations. Depending on the operational experience gained, this change may require activation of all available corrector magnets and thus stronger and/or additional power supplies, but no physical changes of the magnet system will be needed.

The luminosity and the crossing point conditions ( $\beta^*$  values and crossing angle) are interrelated and limited by the magnet apertures, the beam energy, the range of quadrupole power supplies of the insertion, and the available chromaticity sextupoles. Figure 11-8 shows the maximum amplitude function  $\hat{\beta}^{1/2}$  and the chromaticity contribution of one insertion as a function of  $\beta^*$ . Figure 11-9 shows the corresponding quadrupole gradients as a function of  $\beta^*$  at the design tune.

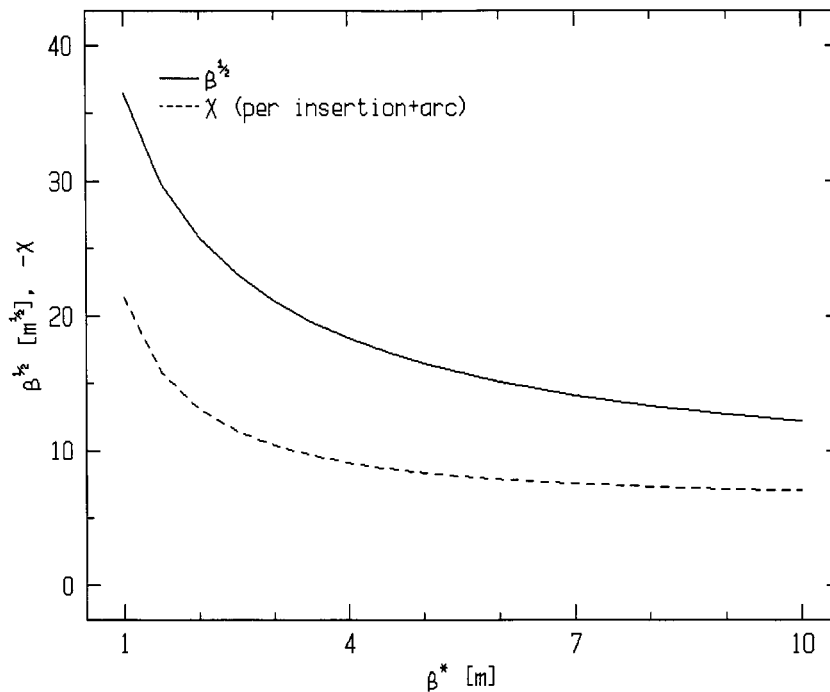


**Fig. 11-8.** The maximum amplitude function and the total natural chromaticity is shown as a function of  $\beta^*$ .

Possible alternative operating tunes range from  $\nu_{H,V} = 27.82$  to 29.20. The tune of the machine can be changed by varying the phase advance in the arc cells as well as the focusing strength of the insertion quadrupoles while maintaining matched conditions. It has been demonstrated that the insertion is tunable over the full  $\beta^*$  range at the following 7 different machine tunes:

$\nu_H =$	28.83	$\nu_V =$	28.82	Equal tune
	28.56		28.55	Half integer tune
	28.83		27.82	Split tune
	29.20		28.20	Split tune
	28.20		28.20	Alternate tune
	28.96		28.95	Integer tune
	28.19		29.18	Nominal tune

The power supplies installed assure that these  $\beta^*$  tune combinations are reachable.

